Journal of Metals, Materials and Minerals, 35(3), e2211, 2025

Oxidation of Sn-1 wt% Bi in air and in oxygen deprived environment

Pakawat POLMANEE[1], Benjie FERNANDEZ[2], Patama VISUTTIPITUKUL[1], Ittipon CHEOWANISH[2], and Tachai LUANGVARANUNT[1,*]

[1] *Department of Metallurgical Engineering, Faculty of Engineering, Chulalongkorn, University, Phayathai Road, Bangkok, 10330, Thailand*
[2] *Department of Slider Development, Thailand Head Operation, Western Digital Storage Technologies (Thailand) Ltd., 140 Moo 2, Udomsorayuth Road, Bangpa-In Ayutthaya 13160, Thailand*

***Corresponding author e-mail**: Tachai.L@chula.ac.th

Received date:
22 November 2024
Revised date:
14 May 2025
Accepted date:
7 June 2025

Keywords:
Electrochemical analysis;
Oxidation of tin;
Thickness of tin oxide film;
X-ray photoelectron microscopy

Abstract

Oxidation of Sn-1wt% Bi in air and in oxygen deprived environment is studied in this research. Electrochemical process with SERA technique was used to determine oxide film thickness and rate of oxidation of tin alloy. The thickness of oxide film at 72 h of the specimens that is tested in air, in vacuum, in argon environment, and wrapped with plastic film are 16 Å, 10 Å, 18 Å, and 13 Å respectively. XPS was used to determine the type of oxides in the oxide layer. Result after signals deconvolution shows that SnO and SnO_2 compounds were formed on the Sn-1wt% Bi surface.

1. Introduction

Hard disks are widely used storage devices and are also an important part of today's cloud technology. One of the key components of a hard disk is the hard disk read/write head, which is one of the key factors in its performance in terms of read/write speed. One of the ways to improve performance of a read/write head is to make its surface to be as smooth as possible, by polishing it with nano-size particle like diamond powder. The polishing uses soft metal, to make a polished disc because it will allow the diamond powder to embed and adhere well to the disc. In most polishing, suspension of free abrasive particles in a solution is continuously supplied in between the lapping plate and the workpiece. Sharp edges of diamond particles polish the workpiece without direct contact between the lapping plate and the workpiece [1]. However, in the case of nano-sized abrasive particles, which are very small and weigh very little, the particles can be easily thrown off the lapping plate during polishing rotation. To solve this problem, the abrasive particle should be strongly embedded on the lapping plate. In the previous research, kinetics of tin oxidation on Sn-1 wt% Bi alloy under the influence of time, temperature and humidity levels have been studied [1]. Formation of tin oxides interferes with the embedding of diamond particles on the lapping plate. So, this research focuses on the prevention of formation of tin oxides under the effect of dry air, inert gas and various oxidation prevention methods, aiming to implement proper storage of tin lapping plate, to reduce oxide formation on lapping plate which will improve its lapping performance.

The study of the thickness of the oxide film will be carried out using a potential difference measurement instrument (Galvanostatic). Constant current density is applied to the sample while measuring its potential, creating a potential versus time plot, in the form of sequential electrochemical reduction analysis (SERA). Being a convenient inexpensive non-destructive approach, SERA is more favorable to be used by a number of researchers than other methods. SERA technique evaluates surface film by applying a small constant cathodic current to a test sample submerged in an electrolyte. For tin samples, the optimal applied current falls within the range of $-30\ \mu A\cdot cm^{-3}$ to $-260\ \mu A\cdot cm^{-3}$ [2-6]. The resulting potential-time curve, known as a chronopotentiogram, shows plateaus representing the reduction of oxides on the sample surface. There are two types of oxides that are found on tin metal which are SnO_2 and SnO [7,8]. X-ray photoelectron spectroscopy (XPS), when combined with ion gun sputtering, serves as a valuable technique for identifying the specific tin oxide species within individual film layers. By analyzing the binding energies of tin (Sn) states, XPS can confirm the oxidation states, and hence composition of tin oxide films [4,9]. This information is crucial for understanding lapping plate properties and optimizing its performance.

The purpose of this research is to determine the oxidation rate of oxidation of tin that undergoes oxidation in deprived oxygen conditions at room temperature.

2. Material and experiment

2.1 Material

Tin lapping plates composition is 99.0 wt% tin (Sn) and 1.0 wt% bismuth (Bi). The dimensions of the tin test samples are 20 mm ×

20 mm × 2 mm. Each sample underwent a polishing process using 400, 600, 800, and 1000 grit SiC paper. Then, the samples were annealed at 200°C for 1 h. After annealing, a final polishing step with 1000 grit SiC paper was performed to remove oxide from the annealing process, followed by thorough washing with deionized water and acetone [10].

2.2 Oxidation test

The reference oxidation test condition is in air having relative humidity between 28% and 35%. The second oxidation test condition is in evacuated desiccator having a pressure of 220 torr. The third oxidation test is in argon atmosphere by putting the samples in an argon-filled desiccator. The fourth oxidation test is wrapped in 9 µm polyvinyl chloride plastic film (M Wrap brand), placed in air having relative humidity between 28% and 35%. Every condition was performed in a temperature range of 25°C to 30°C and for 1, 2, 4, 12, 24, 48, and 72 h. The maximum oxidation test time is limited to 72 h to coincide with the actual storage time of lapping plate in the industry.

Condition	**Atmosphere**	**Humidity / pressure**	**Sample handling**
Air (Reference)	Ambient air	28% to 35% RH	Exposed to air in dehumidifier cabinet
Vacuum	Vacuum desiccator	~220 torr	Sealed in vacuum desiccator
Argon atmosphere	Argon gas	Inert (argon atmosphere)	Stored in argon-purged desiccator
Plastic-wrapped	Ambient air	28% to 35% RH	Wrapped in 9 µm PVC film (M Wrap)

2.3 Sequential electrochemical reduction analysis (SERA)

In each Sequential electrochemical reduction analysis (SERA) experiment, the thickness of the tin oxide film on the samples was measured using a galvanostat (Autolab B.V., Model PGSTAT204). These experiments took place in a 80 mL borate buffer solution containing 6.18 g·L^{-1} boric acid and 9.55 g·L^{-1} sodium tetraborate decahydrate. The tests were conducted under an argon atmosphere. The electrochemical flat cell featured separate compartments for a platinum rod counter electrode, an Ag/AgCl reference electrode, and a glass tube for purging argon gas. A reduction current of –40 µA was continuously applied during the experiments. Details of the SERA setup can be found elsewhere [1].

2.4 X-ray photoelectron spectroscopy (XPS)

X-ray photoelectron spectroscopy (XPS) was performed using the Kratos Axis Ultra DLD instrument with Al Kα radiation. Each specimen underwent the following analyses:

1. Before argon ion etching
2. After argon ion etching for 10 s with 500 eV (for 10 cycles)
3. After argon ion etching for 10 s with 1 keV (for 10 cycles)
4. After argon ion etching for 10 s with 3 keV (for 10 cycles)
5. After argon ion etching for 10 s with 4 keV (for 10 cycles)

These steps allowed characterization of the composition and chemical states at different depths from surface.

3. Results and discussion

3.1 Thickness of oxide film

SERA is used to determine thickness of tin oxide film. Figure 1 shows an example of how zones in the obtained curve are divided for thickness determination. As shown in Figure 1, the curve can be separated into three zones. The first Zone starts with rapid potential drop. It is believed that this potential drop is the reduction of oxide clusters at the outermost layer of the surface [3]. These clusters are likely to be non-uniformed. From this reason, plateau is not found in this part of Zone 1. After this potential drop, the remaining of Zone 1 is a long flat plateau representing reduction of thick oxide film, before the potential starts to drop again. The change in slope of the curve gives the start of Zone 2, it represents reduction of a very thin oxide layer. Zone 2 is not a plateau, but rather a straight portion of the curve, starts and ends with changes of slope. Zone 2 is not a horizontal plateau due to the lack of well defined oxide film. The second change of slope of the curve gives the start of Zone 3. It is where hydrogen evolution from the solution occurs. In earlier research, plateau in Zone 1 represents SnO, and Zone 2 represents not-well-defined SnO_2. The oxide layer in Zone 2 does not show a plateau because it is very thin and incoherent [2,3].

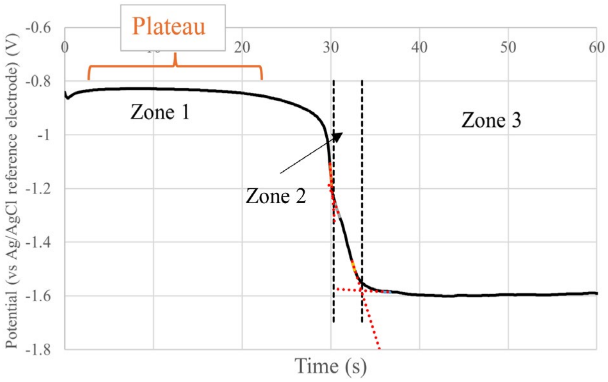

Figure 1. Example of galvanostat result and Zone dividing of a Sn-1% Bi sample.

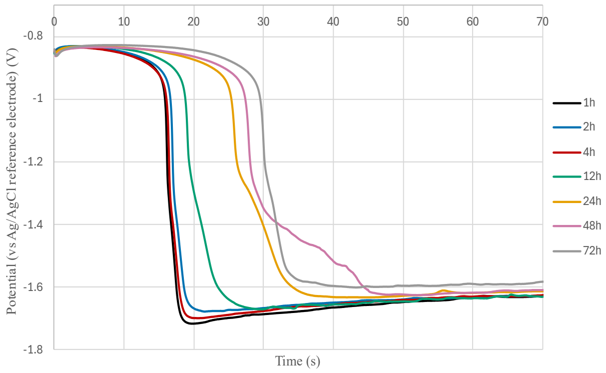

Figure 2. SERA curves of Sn-1 wt% Bi of samples oxidation tested in air at 28% *to* 35% relative humidity.

As shown in Figure 2, for air with 28% to 35% relative humidity condition, as time in oxidation testing increases, the time used to perform SERA increases in both Zone 1 and Zone 2. That means as time in oxidation testing increases, thicker oxide film is formed in both SnO and SnO_2 forms. Calculated thickness of oxide film is shown in Table 2. Details of calculation procedure can be found elsewhere [2-6]. When plotting thickness vs time as in Figure 3, the trend of film thickness behaves like parabolic law in oxidation of metal at high temperatures, of which equation is $y = 8.7041x^{0.14}$. When comparing to a previous research in which tin alloy sample was oxidation tested in air with relative humidity of 29% to 32%, the result was the following equation: $y = 13.90x^{0.14}$ [10]. The slight difference may be due to fluctuation of temperature and humidity between the two researches. For tin metal, room temperature, 298 K, is considered high temperature due to the fact that tin metal has melting temperature at 505 K.

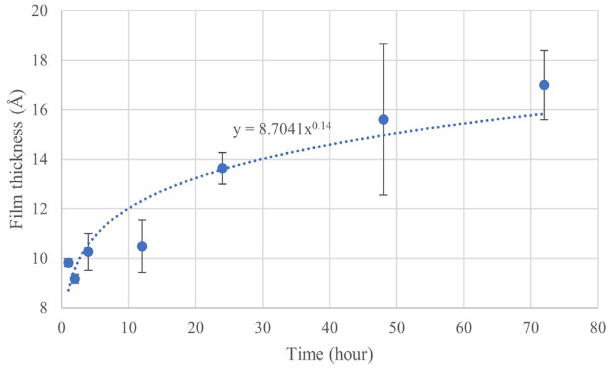

Figure 3. Thickness of film vs time oxidation tested of samples tested in air.

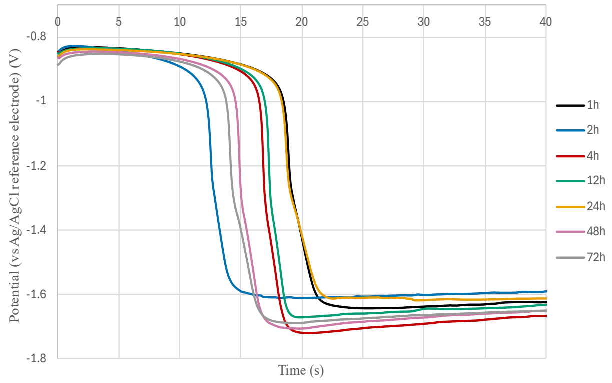

Figure 4. SERA curves of Sn-1 wt% Bi of samples oxidation tested in vacuum.

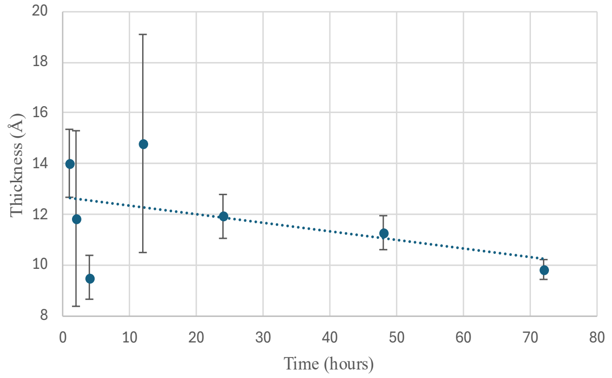

Figure 5. Thickness of film vs time oxidation tested of samples tested in vacuum.

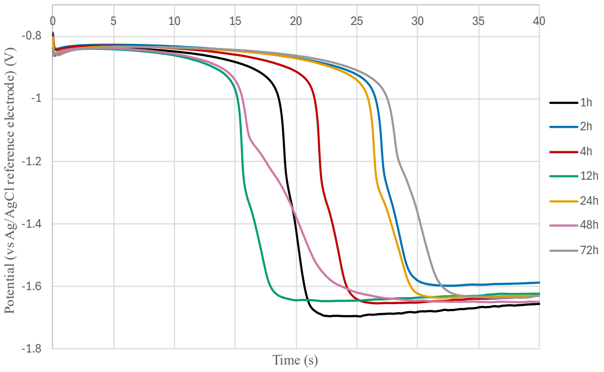

Figure 6. SERA curves of Sn-1 wt% Bi of samples oxidation tested in argon atmosphere.

Table 1. Calculated thickness of oxide film of samples tested in air.

Time	Thickness (Å)		
[h]	Zone 1	Zone 2	Total
1	9.2	0.4	9.6
2	8.8	0.4	9.2
4	9.7	0.5	10.2
12	9.4	0.6	10.0
24	12.5	1.9	14.4
48	12.5	3.8	16.3
72	15.5	0.8	16.3

Table 2. Calculated thickness of oxide film of samples tested in vacuum.

Time	Thickness (Å)		
[h]	Zone 1	Zone 2	Total
1	12.4	0.6	13.0
2	9.6	0.5	10.1
4	9.2	0.3	9.5
12	11.4	0.4	11.8
24	9.9	0.8	10.7
48	10.6	0.5	11.1
72	9.2	0.7	9.9

Table 3. Calculated thickness of oxide film of samples tested in argon atmosphere.

Time	Thickness (Å)		
[h]	Zone 1	Zone 2	Total
1	14.1	0.6	14.7
2	11.3	4.7	16
4	12.3	0.5	12.8
12	11.7	0.6	12.3
24	15.5	0.9	16.4
48	13.4	1.5	14.9
72	17.1	1	18.1

Table 4. Calculated thickness of oxide film of samples tested in plastic wrap.

Time	Thickness (Å)		
[h]	Zone 1	Zone 2	Total
1	10.4	0.8	11.2
2	10.2	0.5	10.7
4	8.2	0.4	8.6
12	10.5	0.6	11.1
24	11.2	1.0	12.2
48	9.5	0.5	10.0
72	12.1	0.5	12.6

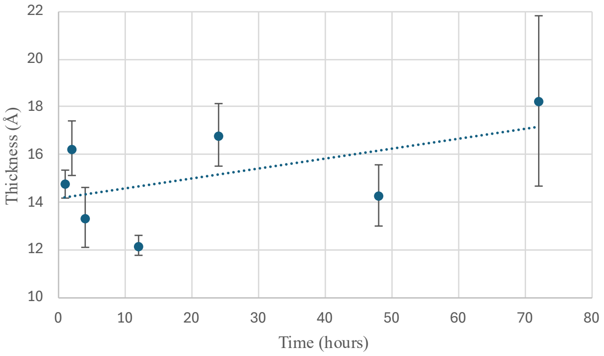

Figure 7. Thickness of film vs time oxidation tested of samples tested in argon atmosphere.

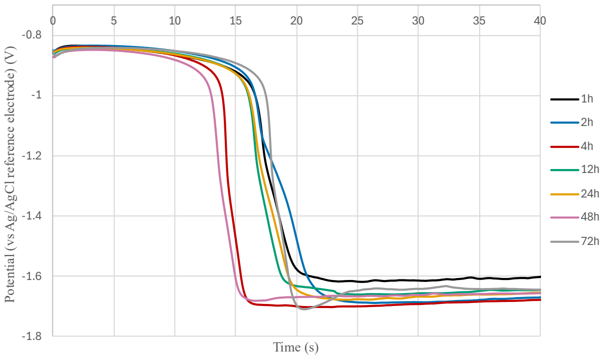

Figure 8. SERA curves of Sn-1 wt% Bi of samples oxidation tested that is wrapped in plastic.

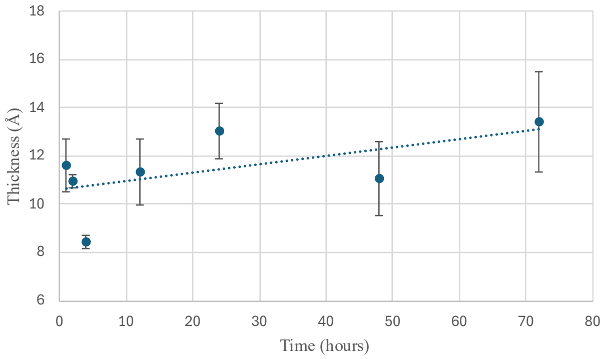

Figure 9. Thickness of film vs time oxidation tested of samples tested in plastic wrap.

In contrast, other oxygen deprived conditions, which are tested in vacuum, in argon environment and wrapped with plastic, the results do not show that oxidation rate would obey parabolic law [11], as shown in Figure 5, Figure 7, and Figure 9. For oxidation in vacuum, the oxides thickness remains relatively constant over the entire test period. However, in some cases, anomalies such as a higher thickness at the 1 h mark were observed. This may be attributed to equipment limitations. The vacuum desiccator used in this study was not specifically designed to maintain a stable vacuum over extended periods. As a result, the internal pressure gradually increased over time and eventually approached ambient atmospheric conditions. In some cases, unintentional setup errors, such as imperfect sealing, may have caused air to enter more rapidly than expected, further compromising the vacuum environment and affecting the oxidation behavior of the samples. Despite these fluctuations, a linear trendline was fitted to the vacuum condition data, resulting in the equation $y = -0.0336x + 12.667$, with a correlation coefficient $R = -0.464$. For oxidation in argon gas and plastic wrap, the oxides thickness gradually increases with time. The fitted linear trendline for argon condition $y = 0.0411x + 14.171$ with $R = 0.532$. In the plastic wrap condition, oxide thickness also increases over time. The linear regression yields $y = 0.0346x + 10.595$ with $R \approx 0.577$. Comparing film thickness of oxidation in air in Table 1 and oxidation in oxygen deprived conditions in Table 2-4 shows that overall oxygen deprived conditions have less oxide film thickness than oxidation in air. The large fluctuation of thickness values of samples placed in argon atmosphere is due to continuous leakage at the desiccator lid. SERA curves of oxygen deprived conditions are shown in Figure 4, Figure 6, and Figure 8, indicating that their reduction times are less than that of oxidation in air.

3.2 Types of oxide

To identify oxide films in this experiment, XPS (X-ray photoelectron spectroscopy) was performed. Specimen oxidation tested in vacuum 72 h was analyzed as stated in 2.3. The signals of Sn 3d are as seen in Figure 10. After deconvolution as shown in Figure 12, there are three peaks for Sn 3d5/2 and three peaks for Sn 3d3/2 which represent Sn0, Sn^{2+} and Sn^{4+}. The binding energy of Sn0, Sn^{2+} and Sn^{4+} for Sn 3d5/2 are 485.25 eV, 486.35 eV and 487.55 eV respectively [2,9]. As the analysis goes deeper, after each argon ion bombarding, signal of Sn0 which is Sn metal becomes stronger, while Sn^{2+} and Sn^{4+} which represent SnO and SnO_2 become weaker as seen in Figure 9-10. However, at the very beginning of ion bombarding, Sn^{4+} signal is greater than Sn^{2+}. This suggests that the outermost part of the surface is indeed SnO_2 cluster, which is quickly removed right after the first 10 s of bombardment. This is in good agreement with the initial potential drop in Zone 1 of the electrochemical analysis. As the analysis goes deeper, SnO and SnO_2 signals are continuously declining. The coexisting of SnO and SnO_2 at this depth is likely due to a transformation of SnO to SnO_2 underneath the SnO layer [2,3,5]. This corresponds to the straight portion in Zone 2 of the electrochemical analysis. Finally, when the specimen is bombarded for the last time (400 s), almost all SnO and SnO_2 signal disappear, and only elemental tin remains.

Concentration of tin and oxygen elements against bombarding time is shown in Figure 13. After 400 s argon ion bombardment, at the finish of XPS analysis, oxygen are nearly completely removed, and most of the element detected is tin.

From electrochemical and XPS results, it can be seen that the formation of oxides layer can be illustrated as in Figure 14. The outmost surface consists of clusters of SnO_2, followed by a well-defined SnO layer, very thin SnO_2 layer, and finally the tin substrate. Formation structure of tin oxides of Sn-1 wt% Bi under oxygen deprived environment is identical to the formation structure of tin oxides of this same material in dry air [1].

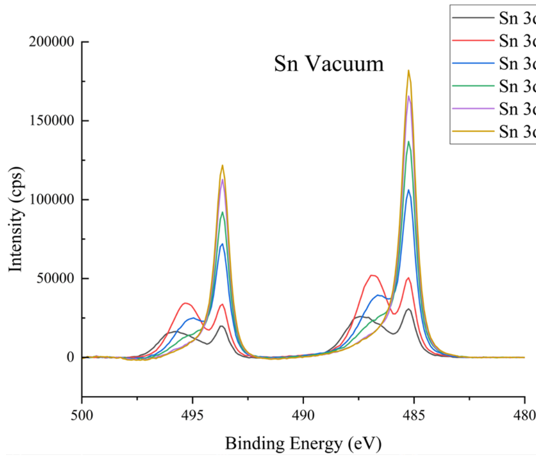

Figure 10. Signal intensity of Sn 3d of a specimen oxidation tested in vacuum for 72 h that Argon ion bombarded 0 s to 400 s.

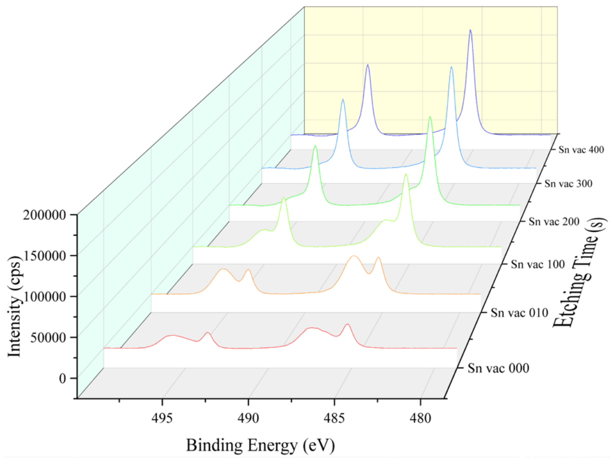

Figure 11. Signal intensity of Sn 3d of a specimen oxidation tested in vacuum for 72 h that Argon ion bombarded 0 s to 400 s in 3D.

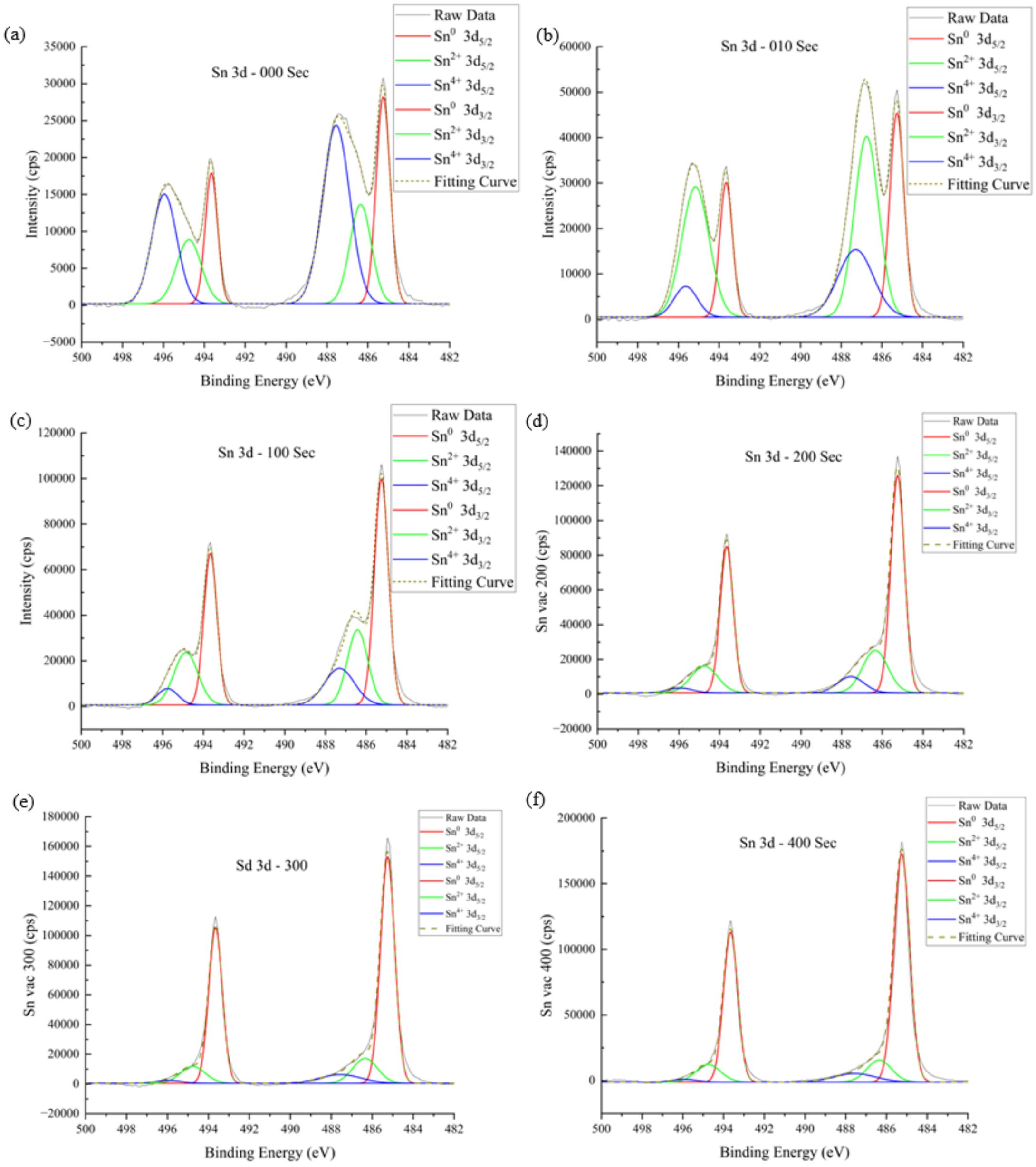

Figure 12. Deconvoluted signal Sn 3d of a specimen oxidation tested in vacuum for 72 h that Argon ion bombarded 0 s to 400 s.

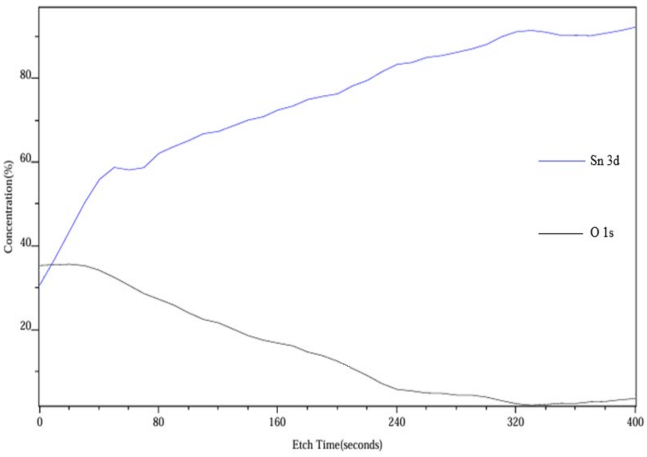

Figure 13. Depth profile of a specimen oxidation tested in vacuum for 72 h.

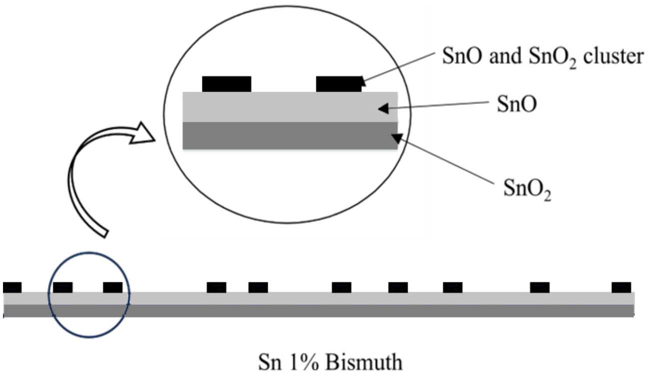

Figure 14. The model predicts the possibility of oxide film formation of tin metal.

4. Conclusion

From the experiment, Sn-1 wt% Bi that are oxidation tested in air and in oxygen deprived environment results in different behavior. The samples that were tested in air at relative humidity between 28% to 35%, the rate of oxidation follow parabolic law, according to classical oxidation of metal at high temperature. The samples that are tested in oxygen deprived environment do not follow parabolic law. For oxidation in vacuum, the oxides thickness remains relatively constant over the entire 72 h test period. For oxidation in argon gas and plastic wrap, the oxides thickness gradually increases with time. Overall, oxide thickness of samples oxidized in air has greater oxide thickness than those tested in oxygen deprived environment. The thickness values of oxide film after 72 h oxidation tests in air, vacuum, argon environment, and wrapped with plastic are 16.39 Å, 9.91 Å, 18.10 Å, and 12.6 Å respectively. From XPS result, after signals deconvolution, it is shown that SnO and SnO_2 are formed on the Sn-1 wt% Bi alloy surface.

Acknowledgements

The authors gratefully acknowledge Western Digital (Thailand) Co., Ltd. for the financial and materials support of the project.

Reference

[1] T. Naravuthichai, P. Visuttipitukul, S. Leelachao, and T. Luangvaranunt, "Oxidation behavior of Sn-1 wt% Bi alloy in air and deionized water at room temperature," *Journal of Metals, Materials and Minerals,* vol. 31, no. 4, pp. 45-50, 2021.

[2] S. Cho, J. Yu, S. K. Kang, and D. Shih, "The oxidation of lead-free Sn alloys by electrochemical reduction analysis," *JOM: the journal of the Minerals, Metals & Materials Society,* vol. 57, no. 6, pp. 50-52, 2005.

[3] D. Hillman, and L. Chumbley, "Characterization of tin oxidation products using sequential electrochemical reduction analysis (SERA)," *Soldering and Surface Mount Technology,* vol. 18, pp. 31-41, 2006.

[4] S. K. Kang, D. Y. Shih, D. Leonard, D. W. Henderson, T. Gosselin, S. I, Cho, J. Yu, and W. K. Choi, "Controlling Ag_3Sn plate formation in near-ternary-eutectic Sn-Ag-Cu solder by minor Zn alloying," *JOM: the journal of the Minerals, Metals & Materials Society*, vol. 56, no. 6, pp.34-38, 2004.

[5] D. M. Tench, D. P. Anderson, and P. Kim, "Solderability assessment via sequential electrochemical reduction analysis," *Journal of Applied Electrochemistry,* vol. 24, no. 1, pp. 18-29, 1994.

[6] A. Rezaie, H. Ghasemi, and F. Eslami, "An in-depth investigation of the impact of salt nature on the formulation of microemulsion systems," *Scientific Reports,* vol. 13, no. 1, p. 14362, 2023.

[7] T. Bring, B. Jonson, L. Kloo, J. Rosdahl, and R. Wallenberg, "Colour development in copper ruby alkali silicate glasses. Part 1. The impact of tin(II) oxide, time and temperature," *Glass Technology: European Journal of Glass Science and Technology Part A,* Article vol. 48, no. 2, pp. 101-108, 2007.

[8] N. N. N. N. Greenwood, "*Chemistry of the elements*," New York: Pergamon Press (in English), 1984.

[9] L. Jie, and X. Chao, "XPS examination of tin oxide on float glass surface," *Journal of Non-Crystalline Solids,* vol. 119, no. 1, pp. 37-40, 1990.

[10] T. Naravuthichai, "*Kinetics of Tin Oxidation Under the Influence of Temperature, Time and Humidity*," Metallurgical Engineering, Chulalongkorn University, Bangkok, 2020.

[11] A. S. Khanna, "Chapter 6 - High temperature oxidation," in *Handbook of Environmental Degradation of Materials*, M. Kutz Ed. Norwich, NY: William Andrew Publishing, 2005, pp. 105-152.